Syntheses of Chromium Pentacarbonyl Derivatives of Arsenic(V) and Antimony(V). Contrasting Chemical Reactivity with Organic Halogen Derivatives

Jiann-Jang Cherng,[†] **Yun-Wen Lai,**[†] **Yi-Hung Liu,**[‡] **Shie-Ming Peng,**[§] **Chuen-Her Ueng,**[†] **and Minghuey Shieh***[,†]

Department of Chemistry, National Taiwan Normal University, Taipei 116, Taiwan, Republic of China,
and Department of Chemistry and Instrumentation Center, National Taiwan University,
Taipei 107, Taiwan, Republic of China

Received April 18, 2000

We have synthesized a new series of chromium−group 15 dihydride and hydride complexes $[H_2As\{Cr(CO)_5\}_2]^-$ (**1**) and $[HE\{Cr(CO)_5\}_3]^{2-}$ (E = As, **2a**; E = Sb, **2b**), which represent the first examples of group 6 complexes containing E−H fragments. The contrasting chemical reactivity of **2a** and **2b** with organic halogen derivatives is demonstrated. The reaction of **2a** with RBr (R = $PhCH_2$, $HC{\equiv}CCH_2$) produces the RX addition products $[(R)(Br)As\{Cr(CO)_5\}_2]^-$ (R = $PhCH_2$, **3**; R = C_3H_3, **4**), while the treatment of **2b** with RX (RX = $PhCH_2Br$ or $HC{\equiv}CCH_2Br$, $CH_3(CH_2)_5C(O)Cl$) forms the halo-substituted complexes $[XSb\{Cr(CO)_5\}_3]^{2-}$ (X = Br, **5**; X = Cl, **6**). Moreover, the dihaloantimony complexes $[XX'Sb\{Cr(CO)_5\}_2]^-$ can be obtained from the reaction of **2b** with the appropriate organic halides. In this study, a series of organoarsenic and antimony chromium carbonyl complexes have been synthesized and structurally characterized and the role of the main group on the formation of the resultant complexes is also discussed.

Introduction

Transition metal carbonyl complexes incorporating main group fragments have attracted great attention because of their unusual bonding and versatile reactivity patterns.[1] In contrast to the well-developed iron−group 15 complexes,[2] most of the previously described As−Cr−CO and Sb−Cr−CO complexes exhibit trigonal-planar structures such as $XAs\{Cr(CO)_5\}_2$ (X = Br, Cl, I, Ph, OMe, OEt, SC_2H_5, SC_6H_{11}, SeC_6H_5)[3] and $ML_nE\{Cr(CO)_5\}_2$ (ML_n = $Mn(CO)_5$, E = As; ML_n = $Cr(CO)_5$, $Mn(CO)_5$, $MoCp(CO)_3$, $Mo(CO)_5$, $W(CO)_5$, E = Sb).[4] We have developed a facile route to a new series of chromium−group 15 dihydride and hydride complexes $[H_2As\{Cr(CO)_5\}_2]^-$ (**1**) and $[HE\{Cr(CO)_5\}_3]^{2-}$ (E = As, **2a**; E = Sb, **2b**). There are relatively few well-characterized metal carbonyl complexes containing E−H (E = As, Sb) fragments, and the structurally authenticated examples are limited to $(\mu\text{-}HAs)\{CpMn(CO)_2\}_2$,[5] $[HAs\{Fe(CO)_4\}_3]^{2-}$,[6,7] and $[HSb\{Fe(CO)_4\}_3]^{2-}$.[7] To our knowledge, complexes **1**, **2a**, and **2b** represent the first examples of group 6 complexes containing E−H fragments in which **2a** and **2b** contain one E−H bond each and **1** possesses two E−H bonds.

The main group element has been shown to have influence on the reactivity of the mixed main group−transition metal complexes in the well-studied E−Fe−CO system.[2g−i,8] To understand the effect of main group elements on this new family of E−Cr−CO complexes, we extensively investigate the chemical reactivity of $[HE(Cr(CO)_5)_3]^{2-}$ (E = As, **2a**; E = Sb, **2b**) with organic halides. In this paper, we report the contrasting chemical reactivity of **2a** and **2b** with organic halogen derivatives, and a series of new organoarsenic and antimony chromium carbonyl complexes (**3**−**8**) has been synthesized and structurally characterized as well. The syntheses of **2a** and **2b** have been communicated.[9]

---

* To whom correspondence should be addressed.

[†] Department of Chemistry, National Taiwan Normal University.

[‡] Instrumentation Center, National Taiwan University.

[§] Department of Chemistry, National Taiwan University.

(1) (a) Shriver, D. F.; Kasez, H. D.; Adams, R. D. *The Chemistry of Metal Cluster Complexes*; VCH Publishers: New York, 1990. (b) Herrmann, W. A. *Angew. Chem., Int. Ed. Engl.* **1986**, *25*, 56. (c) Scherer, O. J. *Comments Inorg. Chem.* **1987**, *6*, 1. (d) Scherer, O. J. *Angew. Chem., Int. Ed. Engl.* **1985**, *24*, 924. (e) Whitmire, K. H. *J. Coord. Chem.* **1988**, *17*, 95. (f) Huttner, G.; Evertz, K. *Acc. Chem. Res.* **1986**, *19*, 406. (g) Vahrenkamp, H. *Adv. Organomet. Chem.* **1983**, *22*, 169. (h) Scherer, O. J. *Angew. Chem., Int. Ed. Engl.* **1990**, *29*, 1104. (i) Cowley, A. H. *J. Organomet. Chem.* **1990**, *400*, 71. (j) Dimaio, A.-J.; Rheingold, A. L. *Chem. Rev.* **1990**, *90*, 169. (k) Compton, N. A.; Errington, R. J.; Norman, N. C. *Adv. Organomet. Chem.* **1990**, *31*, 91. (l) Whitmire, K. H. *J. Cluster Sci.* **1991**, *2*, 231. (m) Whitmire, K. H. J. *Adv. Organomet. Chem.* **1997**, *42*, 1. (n) Shieh, M. *J. Cluster Sci.* **1999**, *10*, 3.

(2) (a) Röttinger, E.; Vahrenkamp, H. *Angew. Chem., Int. Ed. Engl.* **1978**, *17*, 273. (b) Luo, S.; Whitmire, K. H. *Inorg. Chem.* **1989**, *28*, 1424. (c) Whitmire, K. H.; Shieh, M.; Lagrone, C. B.; Robinson, B. H.; Churchill, M. R.; Fettinger, J. C.; See, R. F. *Inorg. Chem.* **1987**, *26*, 2798. (d) Whitmire, K. H.; Leigh, J. S.; Luo, S.-F.; Shieh, M.; Fabiano, M. D. *New. J. Chem.* **1988**, *12*, 397. (e) Luo, S.-F.; Whitmire, K. H. *J. Organomet. Chem.* **1989**, *376*, 297. (f) Arnold, L. J.; Mackay, K. M.; Nicholson, B. K. *J. Organomet. Chem.* **1990**, *387*, 197. (g) Shieh, M.; Liou, Y.; Peng, S.-M.; Lee, G.-H. *Inorg. Chem.* **1993**, *32*, 2212. (h) Shieh, M.; Liou, Y. Jeng. B.-W. *Organometallics* **1993**, *12*, 4926. (i) Shieh, M.; Sheu, C.-M.; Ho, L.-F.; Cherng, J.-J.; Ueng, C.-H.; Peng, S.-M.; Lee, G.-H. *Inorg. Chem.* **1996**, *35*, 5504.

(3) (a) Seyerl, J. V.; Sigwarth, B.; Schmid, H.-G.; Mohr, G.; Frank, A.; Marsili, M.; Huttner, G. *Chem. Ber.* **1981**, *114*, 1392. (b) Huttner, G.; Schmid, H.-G. *Angew. Chem., Int. Ed. Engl.* **1975**, *14*, 433.

(4) Huttner, G.; Weber, U.; Sigwarth, B.; Scheidsteger, O.; Lang, H.; Zsolnai, L. *J. Organomet. Chem.* **1985**, *282*, 331.

(5) Herrmann, W. A.; Koumbouris, B.; Zahn, T.; Ziegler, M. L. *Angew. Chem., Int. Ed. Engl.* **1984**, *23*, 812.

(6) (a) Bachman, R. E.; Miller, S. K.; Whitmire, K. H. *Inorg. Chem.* **1994**, *33*, 2075. (b) Bachman, R. E.; Miller, S. K.; Whitmire, K. H. *Organometallics* **1995**, *14*, 796.

(7) Henderson, P.; Rossignoli, M.; Burns, R. C.; Scudder, M. L.; Craig, D. C. *J. Chem. Soc., Dalton Trans.* **1994**, 1641.

(8) Shieh, M.; Ho, L.-F.; Cherng, J.-J.; Ueng, C.-H.; Peng, S.-M.; Lee, G.-H. *J. Organomet. Chem.* **1999**, *587*, 176.

10.1021/ic0004277 CCC: $20.00

Experimental Section

All reactions were performed under an atmosphere of pure nitrogen using standard Schlenk techniques.[10] Solvents were purified, dried, and distilled under nitrogen prior to use. $Cr(CO)_6$ (Strem), As_2O_3 (WAKO), and Sb_2O_3 (Aldrich) were used as received. Infrared spectra were recorded on a Perkin-Elmer Paragon 500 IR spectrometer as solutions in CaF_2 cells. The ^1H and ^{13}C NMR spectra were taken on a JEOL 400 instrument at 399.78 and 100.53 MHz, respectively. FAB mass spectra were taken on a JEOL SX-102A mass spectrometer. Quantitative analysis of the organic products was performed on a Shimadzu GC-9A instrument and GC Hewlett-Packard 6890 instrument equipped with a Hewlett-Packard 5973 MS selective detector. Elemental analyses of C, H, and N were performed on a Perkin-Elmer 2400 analyzer at the NSC Regional Instrumental Center at National Taiwan University, Taipei, Taiwan.

Syntheses of $[Et_4N][H_2As\{Cr(CO)_5\}_2]$ ($[Et_4N]_2[1]$) and $[Et_4N]_2[HAs\{Cr(CO)_5\}_3]$ ($[Et_4N]_2[2a]$). To a mixture of 5.40 g (96.2 mmol) of KOH, 0.20 g (1.00 mmol) of As_2O_3, and 1.32 g (6.01 mmol) of $Cr(CO)_6$ was added 20 mL of MeOH. After being stirred for 3 days at room temperature, the solution was filtered and an aqueous solution of 1.35 g (6.40 mmol) of Et_4NBr was added, precipitating the orange product. The product was collected by filtration, washed with H_2O, and dried under vacuum. The residue was washed with hexane and extracted with ether to give 0.55 g (0.93 mmol) of $[Et_4N][H_2As\{Cr(CO)_5\}_2]$ (47% based on As). Crystals suitable for X-ray diffraction were grown from hexanes/CH_2Cl_2. IR (ν_{CO}, CH_2Cl_2): 2032 s, 1929 vs, 1881 s cm^{-1}. ^1H NMR (CD_2Cl_2, ppm): δ 0.0 (s, 2H) (chemical shifts not given for $[Et_4N]^+$). Negative ion FABMS: m/z 460.8. Anal. Calcd for $[Et_4N][1]$: C, 36.56; H, 3.75; N, 2.37. Found: C, 36.43; H, 3.66; N, 2.16. The residue was then extracted with THF, and the THF extract was recrystallized from ether/THF to give 0.32 g (0.35 mmol) of $[Et_4N]_2[HAs\{Cr(CO)_5\}_3]$ ($[Et_4N]_2[\mathbf{2a}]$) (18% based on As). IR (ν_{CO}, THF): 2007 vs, 1914 vs, 1847 s cm^{-1}. ^1H NMR (DMSO-d_6, ppm): δ -2.0 (s, 1H) (chemical shifts not given for $[Et_4N]^+$). Anal. Calcd for $[Et_4N]_2[\mathbf{2a}]$: C, 40.80; H, 4.53; N, 3.07. Found: C, 40.50; H, 4.45; N, 3.11. Crystals suitable for X-ray diffraction were grown from ether/CH_2Cl_2.

Synthesis of $[Et_4N]_2[HSb\{Cr(CO)_5\}_3]$ ($[Et_4N]_2[2b]$). To a mixture of 5.39 g (96.0 mmol) of KOH, 0.27 g (0.93 mmol) of Sb_2O_3, and 1.25 g (5.67 mmol) of $Cr(CO)_6$ was added 25 mL of MeOH. After being stirred for 3 days at room temperature, the solution was filtered and an aqueous solution of 1.53 g (5.95 mmol) of Et_4NBr was added, precipitating the orange product. This product was collected by filtration, washed with H_2O, and dried under vacuum. Recrystallization from Et_2O/THF gave 1.41 g (1.47 mmol) of $[Et_4N]_2[HSb\{Cr(CO)_5\}_3]$ ($[Et_4N]_2[\mathbf{2b}]$) (79% based on Sb). IR (ν_{CO}, THF): 2003 vs, 1919 vs, 1860 s cm^{-1}. ^1H NMR (DMSO-d_6, ppm): δ -5.5 (s, 1H) (chemical shifts not given for $[Et_4N]^+$). Anal. Calcd for $[Et_4N]_2[\mathbf{2b}]$: C, 38.81; H, 4.31; N, 2.92. Found: C, 38.51; H, 4.34; N, 2.76. Crystals suitable for X-ray diffraction were grown from ether/THF.

Reaction of $[Et_4N]_2[HAs\{Cr(CO)_5\}_3]$ ($[Et_4N]_2[2a]$) with $PhCH_2Br$. To a solution of 0.35 g (0.38 mmol) of $[Et_4N]_2[\mathbf{2a}]$ in 5 mL of THF was added 0.05 mL (0.42 mmol) of $PhCH_2Br$. The resulting solution was stirred in an ice/water bath for 10 min, then warmed to room temperature, and stirred for another 20 h. The solvent was removed under vacuum, and the organic product−toluene (0.239 mmol, 63% based on $[Et_4N]_2[\mathbf{2a}]$) was quantified and identified by GC and GC/MS. The ether extract was recrystallized with hexane/CH_2Cl_2 to give 0.08 g (0.11 mmol) of the pure compound $[Et_4N][(Br)(PhCH_2)As\{Cr(CO)_5\}_2]$ ($[Et_4N][\mathbf{3}]$) (29% based on $[Et_4N]_2[\mathbf{2a}]$). Crystals suitable for X-ray diffraction were grown from ether/CH_2Cl_2. IR (ν_{CO}, THF): 2056 w, 2037 m, 1942 vs, 1933 vs, sh, 1897 s cm^{-1}. ^1H NMR (DMSO-d_6, 298 K, ppm): δ 7.42, 7.41, 7.29, 7.27, 7.22, 7.20 (m, 5H), 4.11 (s, 2H) (chemical shifts not given for $[Et_4N]^+$). ^{13}C NMR (DMSO-d_6, 298 K, ppm): δ 227.69, 220.42, 141.46, 130.84, 128.99, 127.48, 49.18 (chemical shifts not given for $[Et_4N]^+$). Negative ion FABMS: m/z 628.8. Anal. Calcd for $[Et_4N][\mathbf{3}]$: C, 39.49; H, 3.58; N, 1.84. Found: C, 39.26; H, 3.33; N, 1.85. The residue was then extracted with THF, and the THF extract was recrystallized with hexanes/CH_2Cl_2 to give 0.11 g (0.273 mmol) of the known compound $[Et_4N][BrCr(CO)_5]$[11] (24% based on $[Et_4N]_2[\mathbf{2a}]$). IR (ν_{CO}, THF): 2054 w, 1921 vs, 1862 vs cm^{-1}. Anal. Calcd for $[Et_4N][BrCr(CO)_5]$: C, 38.82; H, 5.01; N, 3.48. Found: C, 38.76; H, 4.97; N, 3.27.

Reaction of $[Et_4N]_2[HAs\{Cr(CO)_5\}_3]$ ($[Et_4N]_2[2a]$) with $HC\equiv CCH_2Br$. To a solution of 0.33 g (0.36 mmol) of $[Et_4N]_2[\mathbf{2a}]$ in 20 mL of THF was added 0.04 mL (0.53 mmol) of $HC\equiv CCH_2Br$. The resulting solution was stirred in an ice/water bath for 20 min, then warmed to room temperature, and stirred for another 2 days. The ether extract was recrystallized with hexane/CH_2Cl_2 to give 0.15 g (0.21 mmol) of the pure compound $[Et_4N][(Br)(C_3H_3)As\{Cr(CO)_5\}_2]$ ($[Et_4N][\mathbf{4}]$) (58% based on $[Et_4N]_2[\mathbf{2a}]$). IR (ν_{CO}, THF): 2058 m, 2046 m, 2038 s, 1972 m, 1943 vs, 1900 s cm^{-1}. ^1H NMR (DMSO-d_6, 298 K, ppm): δ 6.80 (t, 1H, $J = 6.23$ Hz), 5.06 (d, 2H, $J = 6.23$ Hz) (chemical shifts not given for $[Et_4N]^+$). ^{13}C NMR (DMSO-d_6, 298 K, ppm): δ 227.58, 220.21, 204.35, 98.46, 77.92 (chemical shifts not given for $[Et_4N]^+$). Negative ion FABMS: m/z 578.7. Anal. Calcd for $[Et_4N][\mathbf{4}]$: C, 35.61; H, 3.27; N, 1.98. Found: C, 35.29; H, 3.40; N, 1.77. The residue was then extracted with THF, and the THF extract was recrystallized with hexanes/CH_2Cl_2 to give the known compound $[Et_4N][BrCr(CO)_5]$.[11]

Reaction of $[Bu_4N]_2[HSb\{Cr(CO)_5\}_3]$ ($[Bu_4N]_2[2b]$) with $PhCH_2Br$. To a solution of 0.72 g (0.61 mmol) of $[Bu_4N]_2[\mathbf{2b}]$ in 7.5 mL of THF was added 0.08 mL (0.67 mmol) of $PhCH_2Br$. The resulting solution was stirred in an ice/water bath for 20 min, then warmed to room temperature, and stirred for another 2.5 h. The solvent was removed under vacuum, and the organic product−toluene (0.373 mmol, 61% based on $[Bu_4N]_2[\mathbf{2b}]$) was quantified and identified by GC and GC/MS. Then the THF extract was recrystallized with ether/THF to give 0.50 g (0.396 mmol) of the pure compound $[Bu_4N]_2[BrSb\{Cr(CO)_5\}_3]$ ($[Bu_4N]_2[\mathbf{5}]$) (65% based on $[Bu_4N]_2[\mathbf{2b}]$). IR (ν_{CO}, THF): 2012 vs, 1929 vs, 1865 s cm^{-1}. Anal. Calcd for $[Bu_4N]_2[\mathbf{5}]$: C, 44.71; H, 5.75; N, 2.22. Found: C, 44.61; H, 5.82; N, 2.05.

Reaction of $[Et_4N]_2[HSb\{Cr(CO)_5\}_3]$ ($[Et_4N]_2[2b]$) with $HC\equiv CCH_2Br$. To a solution of 0.52 g (0.54 mmol) of $[Et_4N]_2[\mathbf{2b}]$ in 20 mL of THF was added 0.055 mL (0.73 mmol) of $HC\equiv CCH_2Br$. The resulting solution was stirred in an ice/water bath for 20 min, then warmed to room temperature, and stirred for another 4 h. The solvent was removed under vacuum, and the CH_2Cl_2 extract was recrystallized with Et_2O/CH_2Cl_2 to give 0.43 g (0.41 mmol) of the pure compound $[Et_4N]_2[BrSb\{Cr(CO)_5\}_3]$ ($[Et_4N]_2[\mathbf{5}]$) (76% based on $[Et_4N]_2[\mathbf{2b}]$).

Reaction of $[Et_4N]_2[HSb\{Cr(CO)_5\}_3]$ ($[Et_4N]_2[2b]$) with $CH_3(CH_2)_5C(O)Cl$. To a solution of 0.63 g (0.66 mmol) of $[Et_4N]_2[\mathbf{2b}]$ in 7.5 mL of THF was added 0.12 mL (0.78 mmol) of $CH_3(CH_2)_5C(O)Cl$. The resulting solution was stirred in an ice/water bath for 20 min, then the solvent was removed under vacuum. The organic product−$CH_3(CH_2)_5CHO$ (>0.40 mmol, 61% based on $[Et_4N]_2[\mathbf{2b}]$) was quantified and identified by GC and GC/MS. The THF extract was recrystallized with ether/THF to give 0.55 g (0.55 mmol) of the pure compound $[Et_4N]_2[ClSb\{Cr(CO)_5\}_3]$ ($[Et_4N]_2[\mathbf{6}]$) (83% based on $[Et_4N]_2[\mathbf{2b}]$). IR (ν_{CO}, THF): 2012 vs, 1930 vs, 1869 s cm^{-1}. Anal. Calcd for $[Et_4N]_2[\mathbf{6}]$: C, 37.46; H, 4.06; N, 2.82. Found: C, 37.44; H, 4.01; N, 2.69.

Reaction of $[Et_4N]_2[BrSb\{Cr(CO)_5\}_3]$ ($[Et_4N]_2[5]$) with $CH_3C(O)Cl$. To a solution of 0.24 g (0.23 mmol) of $[Et_4N]_2[\mathbf{5}]$ in 20 mL of THF in an ice/water bath was added 0.04 mL (0.56 mmol) of $CH_3C(O)Cl$. The mixture was stirred in an ice/water bath for 30 min and then warmed to room temperature and stirred for 1 day. The resultant solution was filtered to collect the filtrate, and the solvent was removed under vacuum. The residue was extracted with mixed solvents of THF/hexanes = 2:3; the extract was then recrystallized with hexanes/CH_2Cl_2 to give 0.09 g (0.13 mmol) of the pure compound $[Et_4N][Cl_2Sb\{Cr(CO)_5\}_2]$ ($[Et_4N][\mathbf{7}]$) (57% based on $[Et_4N]_2[\mathbf{5}]$). Crystals suitable

---

(9) Cherng, J.-J.; Lee, G.-H.; Peng, S.-M.; Ueng, C.-H.; Shieh, M. *Organometallics* **2000**, *19*, 213.

(10) Shriver, D. F.; Drezdon, M. A. *The Manipulation of Air Sensitive Compounds*; Wiley: New York, 1986.

(11) (a) Abel, E. W.; Butler, I. S.; Reid. J. G. *J. Chem. Soc.* **1963**, 2068. (b) Fischer, E. O.; Öfele, K. *Z. Naturforsch.* **1959**, *14b*, 763. (c) Fischer; E. O.; Öfele, K. *Chem. Ber.* **1960**, *93*, 1156.

Table 1. Crystallographic Data for $[Et_4N][H_2As\{Cr(CO)_5\}_2]$ ($[Et_4N]$[**1**]), $[Et_4N]_2[HSb\{Cr(CO)_5\}_3]$ ($[Et_4N]$[**2b**]), and $[Bu_4N][BrISb\{Cr(CO)_5\}_2]\cdot 0.5CH_2Cl_2$ ($[Bu_4N]$[**8**]$\cdot 0.5CH_2Cl_2$)

	$[Et_4N]$[**1**]	$[Et_4N]$[**2b**]	$[Bu_4N]$[**8**]$\cdot 0.5CH_2Cl_2$
empirical formula	$C_{18}H_{22}AsCr_2NO_{10}$	$C_{31}H_{41}Cr_3N_2O_{15}Sb$	$C_{26.5}H_{37}NO_{10}Cr_2SbIBrCl$
fw	591.28	959.40	997.58
cryst syst	triclinic	orthorhombic	monoclinic
space group	$P\bar{1}$	*Pcnb*	$P2_1/n$
a, Å	8.988(5)	13.224(5)	17.073(3)
b, Å	12.123(4)	23.477(3)	14.288(3)
c, Å	12.4341(21)	26.754(4)	17.074(3)
α, deg	79.769(2)		
β, deg	78.60(3)		110.42(3)
γ, deg	74.15(4)		
V, Å^3	1266.6(8)	8306(3)	3903.3(13)
Z	2	8	4
D(calcd), g cm^{-3}	1.550	1.534	1.698
μ, cm^{-1}	22.0	14.7	31.362
diffractometer	Nonius (CAD4)	Nonius (CAD4)	Nonius (CAD4)
radiation *λ*, Å	0.709 30	0.709 30	0.710 73
temp, °C	25	25	25
2*θ* range, deg	18.46−24.18	20.50−27.88	18.40−21.54
t_{min}/t_{max}	0.53/0.62	0.58/0.72	0.375/0.503
independent reflns ($I > 2\sigma(I)$)	3271	3691	4104
R,[a] R_w[a]	0.048, 0.041	0.057, 0.048	0.036, 0.038

[a] Thefunctions minimized during least-squares cycles were $R = \sum|F_o - F_c|/\sum F_o$ and $R_w = [\sum w(F_o - F_c)^2/\sum w(F_o)^2]^{1/2}$.

Table 2. Crystallographic Data for $[Et_4N]_2[HAs\{Cr(CO)_5\}_3]$ ($[Et_4N]$[**2a**]), $[Et_4N][(Br)(PhCH_2)As\{Cr(CO)_5\}_2]$ ($[Et_4N]$[**3**]), and $[Et_4N][Cl_2Sb\{Cr(CO)_5\}_2]$ ($[Et_4N]$[**7**])

	$[Et_4N]$[**2a**]	$[Et_4N]$[**3**]	$[Et_4N]$[**7**]
empirical formula	$C_{31}H_{41}AsCr_3N_2O_{15}$	$C_{25}H_{27}AsBrCr_2NO_{10}$	$C_{18}H_{20}Cl_2Cr_2NO_{10}Sb$
fw	912.58	760.31	707.00
cryst syst	monoclinic	monoclinic	orthorhombic
space group	$P2_1/n$	*C*2/*c*	$Pna2_1$
a, Å	13.4332(3)	21.5470(30	11.9041(3)
b, Å	13.8294(4)	12.39990(10)	13.1714(4)
c, Å	22.4643(6)	23.5648(3)	35.6497(7)
β, deg	92.410(1)	100.1770(10)	
V, Å^3	4169.6(2)	6197.00(13)	5589.6(2)
Z	4	8	8
D(calcd), g cm^{-3}	1.454	1.630	1.680
μ, cm^{-1}	16.18	31.02	19.61
diffractometer	SMART CCD	SMART CCD	SMART CCD
radiation *λ*, Å	0.710 73	0.710 73	0.710 73
temp, °C	22	−123	23
θ range, deg	1.73−23.26	1.76−25.00	1.14−25.00
independent reflns	5991 ($R_{int} = 0.0476$)	5465 ($R_{int} = 0.0289$)	4912 ($R_{int} = 0.0334$)
goodness-of-fit on F^2	1.050	1.041	1.146
R1[a]/wR2[b] [$I > 2\sigma(I)$]	0.0496/0.1097	0.0289/0.0681	0.0396/0.0998
R1[a]/wR2[b] (all data)	0.0878/0.1306	0.0437/0.0762	0.0451/0.1098

[a] $R1 = \sum||F_o| - |F_c||/\sum|F_o|$. [b] $wR2 = [\sum[w(F_o^2 - F_c^2)^2]/\sum[w(F_o^2)^2]]^{1/2}$.

for X-ray diffraction were grown from hexanes/CH_2Cl_2. IR (ν_{CO}, THF): 2065 m, 2043 s, 1950 vs cm^{-1}. Negative ion FABMS: *m*/*z* 576.6. Anal. Calcd for $[Et_4N]$[**7**]: C, 30.58; H, 2.85; N, 1.98. Found: C, 30.68; H, 2.87; N, 1.96. The residue was then extracted with CH_2Cl_2, and the CH_2Cl_2 extract was recrystallized with hexanes/CH_2Cl_2 to give 0.05 g (0.11 mmol) of the known compound $[Et_4N][ClCr(CO)_5]$.[11] IR (ν_{CO}, THF): 2060 w, 1923 vs, 1856 m cm^{-1}. Anal. Calcd for $[Et_4N][ClCr(CO)_5]$: C, 43.65; H, 5.63; N, 3.92. Found: C, 43.65; H, 5.62; N, 3.80.

Reaction of $[Bu_4N]_2[BrSb\{Cr(CO)_5\}_3]$ ($[Bu_4N]_2$[5]) with CH_2I_2. To a solution of 0.51 g (0.40 mmol) of $[Bu_4N]_2$[**5**] in 20 mL of THF in an ice/water bath was added 0.1 mL (1.24 mmol) of CH_2I_2. The mixture was stirred in an ice/water bath for 10 min and then warmed to room temperature and stirred for 4 days. The resultant solution was filtered to collect the filtrate, and the solvent was removed under vacuum. The residue was extracted with mixed solvents of ether/hexanes = 2:1; the extract was then recrystallized with hexanes/CH_2Cl_2 to give 0.23 g (0.24 mmol) of the pure compound $[Bu_4N][BrISb\{Cr(CO)_5\}_2]$ ($[Bu_4N]$[**8**]) (60% based on $[Bu_4N]_2$[**5**]). Crystals suitable for X-ray diffraction were grown from hexanes/CH_2Cl_2. IR (ν_{CO}, THF): 2061 m, 2042 s, 1950 vs, 1920 s cm^{-1}. Negative ion FABMS: *m*/*z* 712.7. Anal. Calcd for $[Bu_4N]$[**8**]: C, 31.91; H, 3.74; N, 1.40. Found: C, 31.92; H, 3.68; N, 1.35. The residue was then extracted with CH_2Cl_2, and the extract was then recrystallized with hexanes/CH_2Cl_2 to give the known compound $[Bu_4N][ICr(CO)_5]$.[11] IR (ν_{CO}, THF): 2052 w, 1922 vs, 1865 s cm^{-1}. Anal. Calcd for $[Bu_4N][ICr(CO)_5]$: C, 44.93; H, 6.46; N, 2.49. Found: C, 44.89; H, 6.26; N, 2.53.

X-ray Structural Characterization of Complexes $[Et_4N]$[1], $[Et_4N]_2$[2a], $[Et_4N]_2$[2b], $[Et_4N]$[3], $[Et_4N]$[7], and $[Bu_4N]$[8]. A summary of selected crystallographic data for $[Et_4N]$[**1**], $[Et_4N]_2$[**2a**], $[Et_4N]_2$[**2b**], $[Et_4N]$[**3**], $[Et_4N]$[**7**], and $[Bu_4N]$[**8**] is given in Tables 1 and 2. Data collection for $[Et_4N]$[**1**], $[Et_4N]_2$[**2b**], and $[Bu_4N]$[**8**] was carried out on a Nonius CAD-4 diffractometer using graphite-monochromated Mo Kα radiation at 25 °C employing the $\theta/2\theta$ scan mode. A ψ-scan absorption correction was made.[12] Data reduction and structural refinement were performed using the NRCC-SDP-VAX packages,[13] and atomic scattering factors were taken from ref 14. Data

---

[12] North, A. C. T.; Philips, D. C.; Mathews, F. S. *Acta Crystallogr.* **1968**, *A24*, 351.

[13] Gabe, E. J.; Le Page, Y.; Charland, J. P.; Lee, F. L.; White, P. S. *J. Appl. Crystallogr.* **1989**, *22*, 384.

Table 3. Selected Bond Distances (Å) and Bond Angles (deg) for $[Et_4N][H_2AsCr_2\{(CO)_5\}_2]$ ([Et$_4$N][**1**])

(A) Distances			
As−Cr(1)	2.518(2)	As−Cr(2)	2.515 (1)
(B) Angles			
Cr(1)−As−Cr(2)	133.86(5)	H(1)−As−H(2)	89.56(4)
Cr(1)−As−H(1)	101.87(5)	Cr(1)−As−H(2)	99.91(5)
Cr(2)−As−H(1)	114.59(5)	Cr(2)−As−H(2)	107.36(5)

Table 4. Selected Bond Distances (Å) and Bond Angles (deg) for $[Et_4N]_2[HAsCr_3\{(CO)_5\}_3]$ ([Et$_4$N][**2a**])

(A) Distances			
As−H	1.58(4)	As−Cr(1)	2.6120(10)
As−Cr(2)	2.6151(11)	As−Cr(3)	2.6127(11)
(B) Angles			
H−As−Cr(1)	100.9(13)	H−As−Cr(2)	101.2(13)
H−As−Cr(3)	98.0(12)	Cr(1)−As−Cr(2)	116.60(4)
Cr(1)−As−Cr(3)	117.90(4)	Cr(2)−As−Cr(3)	116.61(4)

Table 5. Selected Bond Distances (Å) and Bond Angles (deg) for $[Et_4N]_2[HSbCr_3\{(CO)_5\}_3]$ ([Et$_4$N][**2b**])

(A) Distances			
Sb−Cr(1)	2.727(2)	Sb−Cr(2)	2.741(2)
Sb−Cr(3)	2.738(2)		
(B) Angles			
H(1)−Sb−Cr(1)	95.42(5)	H(1)−Sb−Cr(2)	103.83(5)
H(1)−Sb−Cr(3)	101.57(5)	Cr(1)−Sb−Cr(2)	116.79(6)
Cr(1)−Sb−Cr(3)	116.86(7)	Cr(2)−Sb−Cr(3)	116.98(7)

Table 6. Selected Bond Distances (Å) and Bond Angles (deg) for $[Et_4N][(Br)(PhCH_2))As\{Cr(CO)_5\}_2]$ ([Et$_4$N][**3**])

(A) Distances			
As(1)−Cr(1)	2.5071(6)	As(1)−Cr(2)	2.5115(5)
As(1)−Br(1)	2.4081(4)	As(1)−C(11)	2.001(3)
C(11)−C(12)	1.495(4)		
(B) Angles			
Cr(1)−As(1)−Cr(2)	124.00(2)	C(11)−As(1)−Br(1)	95.11(9)
Br(1)−As(1)−Cr(1)	106.12(5)	Br(1)−As(1)−Cr(2)	108.16(2)
C(11)−As(1)−Cr(1)	114.51(9)	C(11)−As(1)−Cr(2)	105.18(8)

Table 7. Selected Bond Distances (Å) and Bond Angles (deg) for $[Et_4N][Cl_2Sb\{Cr(CO)_5\}_2]$ ([Et$_4$N][**7**])

(A) Distances			
Sb(1)−Cl(1)	2.441(4)	Sb(1)−Cl(2)	2.419(4)
Sb(1)−Cr(1)	2.582(2)	Sb(1)−Cr(2)	2.587(2)
(B) Angles			
Cr(1)−Sb(1)−Cr(2)	129.01(6)	Cl(1)−Sb(1)−Cl(2)	93.7(2)
Cl(1)−Sb(1)−Cr(1)	107.2(1)	Cl(1)−Sb(1)−Cr(2)	107.7 (1)
Cl(2)−Sb(1)−Cl(1)	107.1(1)	Cl(2)−Sb(1)−Cr(2)	106.5(1)

Table 8. Selected Bond Distances (Å) and Bond Angles (deg) for $[Bu_4N][BrISb\{Cr(CO)_5\}_2]\cdot 0.5CH_2Cl_2$ ([Bu$_4$N][**8**]·0.5CH$_2$Cl$_2$)

(A) Distances			
Sb−Br	2.697(1)	Sb−I	2.7974(8)
Sb−Cr(1)	2.621 (1)	Sb−Cr(2)	2.627(1)
(B) Angles			
Cr(1)−Sb−Cr(2)	132.96(4)	I−Sb−Br	93.02(3)
Br−Sb−Cr(1)	104.11(4)	Br−Sb−Cr(2)	105.90(4)
I−Sb−Cr(1)	106.23(3)	I−Sb−Cr(2)	107.44(3)

collection for [Et$_4$N]$_2$[**2a**], [Et$_4$N][**3**], and [Et$_4$N][**7**] was carried out on a SMART CCD diffractometer. A SADABS scan absorption correction was made,[15] and all calculations were performed using SHELXTL packages.[16]

Structures of [Et$_4$N][1], [Et$_4$N]$_2$[2a], [Et$_4$N]$_2$[2b], [Et$_4$N][3], [Et$_4$N]-[7], and [Bu$_4$N][8]·0.5CH$_2$Cl$_2$. The crystal of [Et$_4$N][**1**] chosen for diffraction measurement was ca. 0.50 mm × 0.15 mm × 0.12 mm. The crystal of [Et$_4$N]$_2$[**2a**] had dimensions 0.38 mm × 0.25 mm × 0.05 mm. The crystal of [Et$_4$N]$_2$[**2b**] had dimensions 0.35 mm × 0.30 mm × 0.30 mm. The crystal of [Et$_4$N][**3**] had dimensions 0.25 mm × 0.20 mm × 0.20 mm. The crystal of [Et$_4$N][**7**] had dimensions 0.40 mm × 0.35 mm × 0.30 mm, and the crystal of [Bu$_4$N][**8**]·0.5CH$_2$Cl$_2$ had dimensions 0.40 mm × 0.30 mm × 0.20 mm. Cell parameters were obtained from 25 reflections with 2θ angle in the range 18.46−24.18° for [Et$_4$N][**1**], $20.5° < 2\theta < 27.88°$ for [Et$_4$N]$_2$[**2b**], $18.4° < 2\theta < 21.54°$ for [Bu$_4$N][**8**]·0.5CH$_2$Cl$_2$, $1.73° < \theta < 23.26°$ for [Et$_4$N]$_2$-[**2a**], $1.76° < \theta < 25.00°$ for [Et$_4$N][**3**], and $1.14° < \theta < 25.00°$ for [Et$_4$N][**7**]. A total of 3271 reflections with $I > 2.5\sigma(I)$ for [Et$_4$N][**1**] (5991 reflections with $I > 2.0\sigma(I)$ for [Et$_4$N]$_2$[**2a**], 3691 reflections with $I > 2.0\sigma(I)$ for [Et$_4$N]$_2$[**2b**], 5163 reflections with $I > 2.0\sigma(I)$ for [Et$_4$N]-[**3**], 4827 reflections with $I > 2.0\sigma(I)$ for [Et$_4$N][**7**], and 4104 reflections with $I > 2.0\sigma$(I) for [Bu$_4$N][**8**]·0.5CH$_2$Cl$_2$) were refined by least-squares cycles. All the non-hydrogen atoms were refined with anisotropic temperature factors. For [Et$_4$N][**1**], the dihydrides were found from Fourier difference maps, approximately 1.600 Å from the As atom, but not refined in the least-squares cycle. For [Et$_4$N][**2a**], the hydride was located crystallographically and refined isotropically, while for [Et$_4$N][**2b**], the hydride was found from Fourier difference maps, approximately 1.799 Å from the Sb atom, but not refined in the least-squares cycle. Full-matrix least-squares refinement led to convergence with $R = 4.9\%$ and $R_w = 4.2\%$ for [Et$_4$N][**1**], with R1 = 4.96% and wR2 = 10.97% for [Et$_4$N]$_2$[**2a**], with $R = 5.6\%$ and $R_w = 4.7\%$ for [Et$_4$N]$_2$[**2b**], with R1 = 2.89% and wR2 = 6.81% for [Et$_4$N][**3**], with R1 = 3.69% and wR2 = 9.98% for [Et$_4$N][**7**], and with $R = 3.6\%$ and $R_w = 3.8\%$ for [Bu$_4$N][**8**]·0.5CH$_2$Cl$_2$.

The selected bond distances and angles for [Et$_4$N][**1**], [Et$_4$N]$_2$[**2a**], [Et$_4$N]$_2$[**2b**], [Et$_4$N][**3**], [Et$_4$N][**7**], and [Bu$_4$N][**8**]·0.5CH$_2$Cl$_2$ are represented in Tables 3−8, respectively. Additional crystallographic data are available as Supporting Information.

Results and Discussion

Syntheses of the Hydrido Complexes 1, 2a, and 2b. Chromium hexacarbonyl can react with As_2O_3 in concentrated methanolic KOH solution to give the chromium−arsenic dihydrido complex $[H_2As\{Cr(CO)_5\}_2]^-$ (**1**) as the major product and the monohydrido complex $[HAs\{Cr(CO)_5\}_3]^{2-}$ (**2a**) as the minor product. Under similar conditions, the reaction with Sb_2O_3 only yields the monohydrido complex $[HSb\{Cr(CO)_5\}_3]^{2-}$ (**2b**); however, the dihydrido complex $[H_2Sb\{Cr(CO)_5\}_2]^-$ is not observed. This can be rationalized that the larger size of Sb could favor the three chromium substituents to bind more than for As where two chromium substituents may be accommodated easily but three are sterically less favorable. The anionic complexes **1**, **2a**, and **2b** can be isolated as the $[Et_4N]^+$ salts by metathesis, and they are fully characterized by single-crystal X-ray analyses and/or spectroscopic methods. Complex **1** can be viewed as a central As(V) ion coordinated to two $Cr(CO)_5{}^{2-}$ groups and two hydrides. Similarly, complexes **2** and **3** are described as a central As(V) or Sb(V) ion each bonded to three $Cr(CO)_5{}^{2-}$ groups and one hydride.

The most interesting feature of **1**, **2a**, and **2b** is the presence of the hydrides bound to the main group atom. They can be located from the difference maps of the X-ray analyses and are also inferred on the basis of electron-counting considerations, and, most importantly, from ^{1}H NMR data analysis. The ^{1}H NMR spectra exhibit singlets at δ 0.0 for $[H_2As\{Cr(CO)_5\}_2]^-$ (**1**), δ −2.0 for $[HAs\{Cr(CO)_5\}_3]^{2-}$ (**2a**), and δ −5.5 for $[HSb\{Cr(CO)_5\}_3]^{2-}$ (**2b**). These results indicate that the hydridic character of the hydrogens increases in the order of **1** < **2a** < **2b** attributable to the increased negative charge of the complexes

---

(14) *International Tables for X-ray Crystallography*; Kynoch Press: Birmingham, England, 1974; Vol. IV.

(15) Sheldrick, G. M. *SADABS, Siemens Area Detector Absorption Correction Program*; University of Göttingen: Göttingen, Germany, 1996.

(16) Sheldrick, G. M. *SHELXTL, Program for Crystal Structure Detection*; Siemens Analytical X-ray Instruments Inc.: Madison, WI, 1994.

Scheme 1

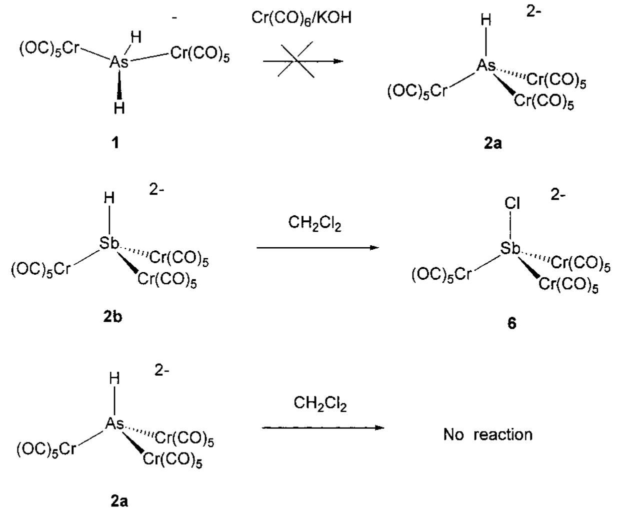

Scheme 2

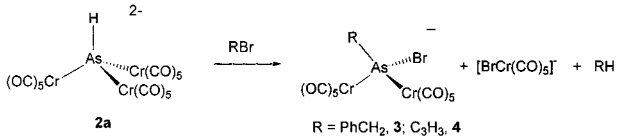

and the increased acidity from As to Sb. Moreover, the values for the monohydrido complexes (**2a** and **2b**) are different from those in the isoelectronic iron complexes $[HAs\{Fe(CO)_4\}_3]^{2-}$ (δ 1.34) and $[HSb\{Fe(CO)_4\}_3]^{2-}$ (δ −1.39).[7] This implies that these hydrogens in chromium-containing complexes **2a** and **2b** are more hydridic than those in the corresponding iron complexes because of the more electropositive character of Cr.

General Reactivity of 1, 2a, and 2b. Is the dihydrido complex **1** an intermediate for the formation of the monohydrido complex **2a**? To answer this, we treated **1** with $Cr(CO)_6$/KOH under controlled conditions. However, **1** was not transformed into **2a**. Therefore, complexes **1** and **2a** result from different reaction pathways. Interestingly, while the hydridoantimony complex **2b** was found to form the chloroantimony complex $[ClSb\{\{Cr(CO)_5\}_3]^{2-}$ (**6**) in CH_2Cl_2 solutions, the hydridoarsenic complex **2a** was not transformed to the corresponding chloroarsenic complex in CH_2Cl_2 solutions (Scheme 1).

Reactions of 2a and 2b with RX. Knowing that the hydride atom of **2b**, but not **2a**, can be easily replaced by chloride in CH_2Cl_2 solutions, we systematically compared the chemical reactivity of **2a** and **2b** with organic halogen derivatives.

In the As−Cr system, surprisingly, complex **2a** was found to react with RBr (R = $PhCH_2$, $HC\equiv CCH_2$), via the formation of the As−R and As−Br bonds, to give the RX addition products $[(R)(Br)As\{Cr(CO)_5\}_2]^-$ (R = $PhCH_2$, **3**; R = C_3H_3, **4**) along with $[BrCr(CO)_5]^-$ (Scheme 2). In the former case, the hydrogen-transferred organic product RH−toluene was also detected and identified by GC and GC/MS. The yield of RH is around 60% based on **2a**. However, the detailed mechanism for the formation of R−H is not clear and may occur via hydride transfer[17] or single electron-transfer processes.[18] Further study is required to understand the mechanistic details.

Scheme 3

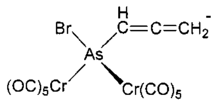

Complex **4** in solution

Scheme 4

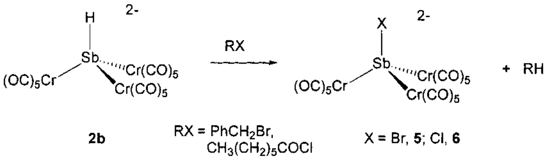

Complexes **3** and **4** were shown to have the tetrahedral (R)(X)$AsCr_2$ core geometry based on spectroscopic data, and the structure of **3** was further characterized by the single-crystal X-ray diffraction method. Note that the C_3H_3 ligand of **4** in solution is of the η^1-allenyl type of ligation according to the ^1H NMR data (two resonances at 6.80 (t, 1H, J = 6.23 Hz) and 5.06 (d, 2H, J = 6.23 Hz)) (Scheme 3).[19]

In the Sb−Cr system, the reactions of **2b** with RX (RX = $PhCH_2Br$ or $HC\equiv CCH_2Br$, $CH_3(CH_2)_5C(O)Cl$), however, gave the haloantimony complexes $[XSb\{Cr(CO)_5\}_3]^{2-}$ (X = Br, **5**; X = Cl, **6**). The corresponding hydrogen-transferred organic products RH (R = $PhCH_2$, $CH_3(CH_2)_5C(O)$) have been characterized and quantified by GC and GC/MS spectroscopy (Scheme 4). Note that the yields of the hydrogen-transferred product RH in both cases are around 60% based on **2b**, close to that found in the As−Cr system and indicative of the comparable hydrogen-transferring efficiency of **2a** and **2b**.

From the above-mentioned results, the contrasting chemical reactivity of complexes **2a** and **2b** toward organic halides is evident. While complex **2a** produces the RX addition products, complex **2b** gives the X-substituted products. The size effect of As and Sb could be taken into account in terms of toleration of the negative charge of the resultant complexes. The RX addition products **3** and **4** each bear only one negative charge, which can be stabilized by the smaller As atom, whereas the haloantimony complexes **5** and **6** each possess two negative charges that are better stabilized by the larger Sb atom. However, on the basis of the yields of formation of R−H, the hydrogen transferring efficiency of **2a** and **2b** is about the same and cannot be distinguishable under our conditions, although the ^1H NMR chemical shifts indicate that the hydrogen atom of **2b** is more hydridic than that of **2a**.

Mixed Dihaloantimony Complexes. Different halides can be introduced into **2b**. The bromoantimony complex **5** can be produced from **2b** with $PhCH_2Br$. The mixed dihaloantimony complex $[BrISb\{Cr(CO)_5\}_2]^-$ (**8**) can be obtained from the further reaction of complex **5** with CH_2I_2. These dihaloantimony complexes may form via the formation of the intermediate halostibinidene complex $[XSb\{Cr(CO)_5\}_2]$ followed by the attack of the incoming halide. This assumption is consistent with the fact that the chloroarsinidene complex $[ClAs\{Cr(CO)_5\}_2]$ can be attacked by Lewis bases to form the adduct.[20] However, if complex **5** were treated with $CH_3C(O)Cl$, a dichloroantimony complex $[Cl_2Sb\{Cr(CO)_5\}_2]^-$ (**7**) would be obtained instead of the expected mixed bromochloroantimony complex. The results

---

(17) (a) Kao, S. C.; Darensbourg, M. Y. *Organometallics* **1984**, *3*, 646. (b) Kao, S. C.; Gaus, P. L.; Youngdahl, K.; Darensbourg, M. Y. *Organometallics* **1984**, *3*, 1601.

(18) Kochi, J. K. *Organometallic Mechanisms and Catalysis*; Academic Press: New York, 1978.

(19) Keng, R.-S.; Lin, Y.-C. *Organometallics* **1990**, *9*, 289 and references therein.

(20) von Seyerl, J.; Huttner, G. *Angew. Chem., Int. Ed. Engl.* **1979**, *18*, 233.

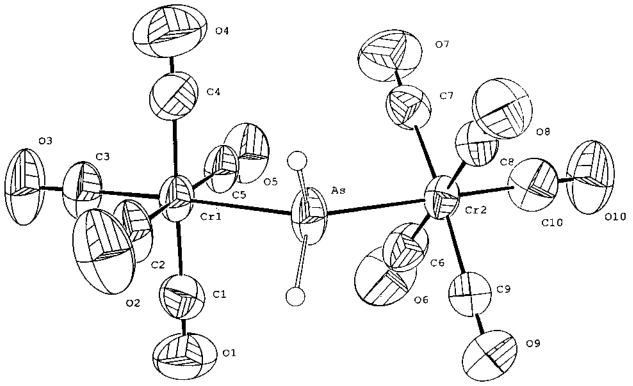

Figure 1. ORTEP diagram showing the structure and atom labeling for the anion **1**.

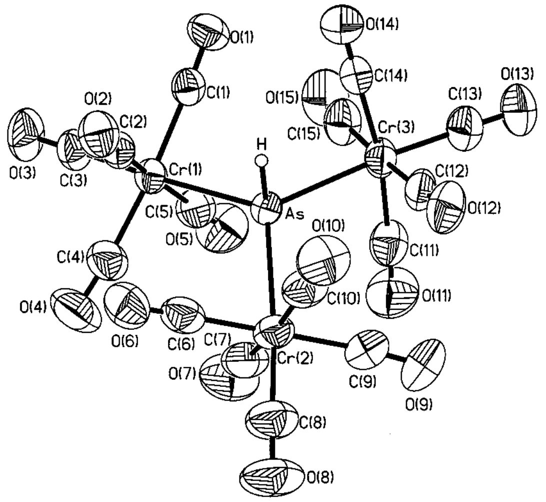

Figure 2. ORTEP diagram showing the structure and atom labeling for the dianion **2a**.

Scheme 5

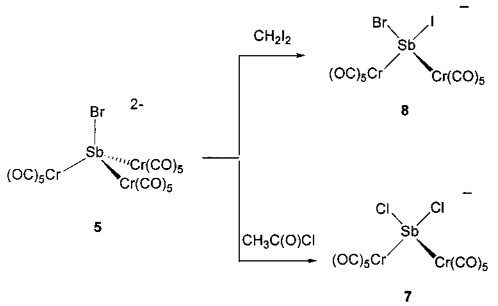

indicate that the formation of mixed dihaloantimony complexes could result from other complicated pathways and that the outcome strongly depends on the reactivity of the incoming organic halides (Scheme 5).

Complexes 1−8. All the new complexes **1**−**8** are fully characterized by spectroscopic methods and/or by X-ray analysis. The structures of [Et$_4$N][**1**] (Figure 1), [Et$_4$N]$_2$[**2a**] (Figure 2), [Et$_4$N]$_2$[**2b**] (Figure 3), [Et$_4$N][**3**] (Figure 4), [Et$_4$N][**7**] (Figure 5), and [Bu$_4$N][**8**] (Figure 6) are further determined by single-crystal X-ray diffraction in which the central atoms (As or Sb) are all in distorted tetrahedral environments. The analyses show that the dianionic complexes **2a**, **2b**, **5**, and **6** each consist of a central antimony(V) or arsenic(V) ion tetrahedrally coordinated to one hydride (or halide) and three Cr(CO)$_5^{2-}$ groups. The monoanions **1** and **7** (or **8**) are structurally similar to the dianionic **2a** or **6** (or **5**) except that one Cr(CO)$_5^{2-}$ group is replaced by another hydride or halide, respectively. Similarly, the monoanions **3** and **4** each display a central arsenic(V) ion bonded to two Cr(CO)$_5^{2-}$ groups, one organic R$^-$ group, and one bromide moiety.

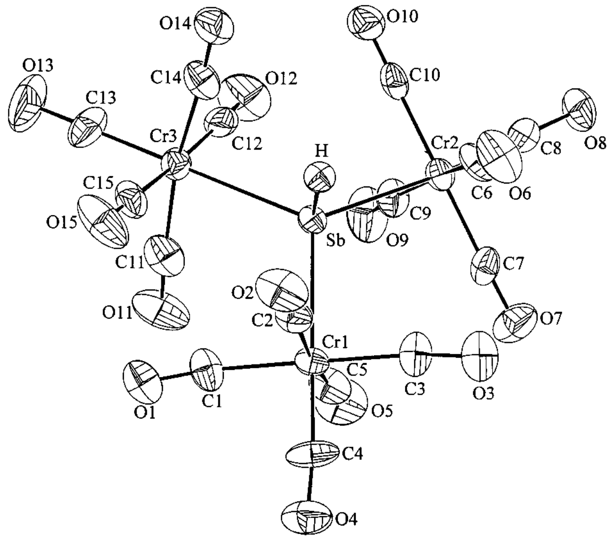

Figure 3. ORTEP diagram Showing the structure and atom labeling for the dianion **2b**.

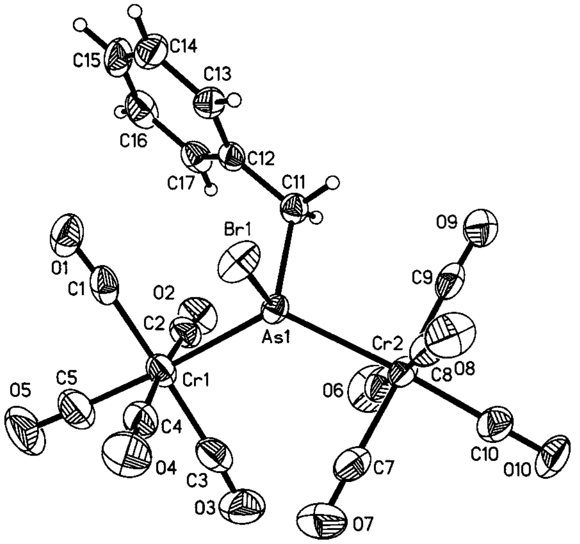

Figure 4. ORTEP diagram showing the structure and atom labeling for the anion **3**.

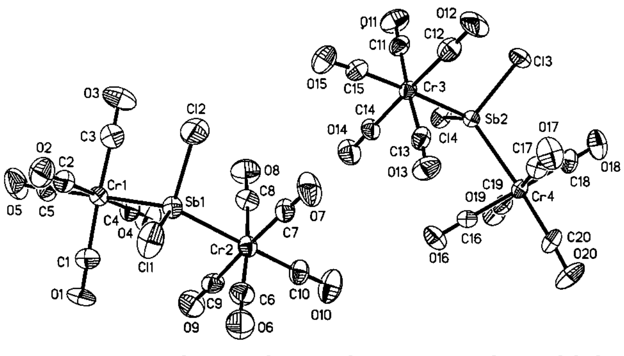

Figure 5. ORTEP diagram showing the structure and atom labeling for the anion **7**.

For comparison, the average Cr−E−Cr angle and the E−Cr distance in these tetrahedral complexes are listed in Table 9. Of the As−Cr complexes **1**, **2a**, and **3**, the average As−Cr

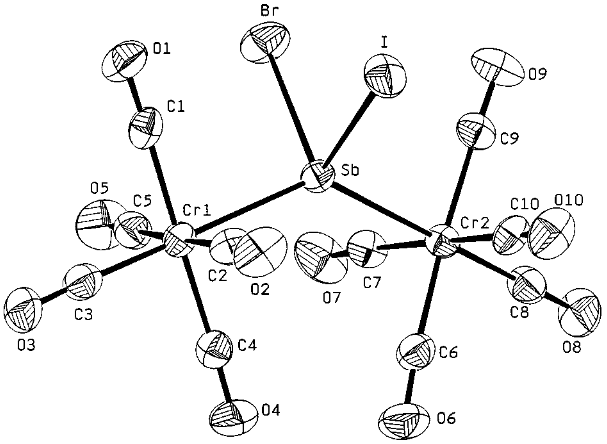

Figure 6. ORTEP diagram showing the structure and atom labeling for the anion **8**.

Table 9. Comparison of the Average Cr−E−Cr Angles and the Average E−Cr Distances in **1**, **2a**, **2b**, **3**, **7**, and **8**

complex	Cr−E−Cr, deg	E−Cr, Å
$[H_2As\{Cr(CO)_5\}_2]^-$ (**1**)	133.86	2.516
$[HAs\{Cr(CO)_5\}_3]^{2-}$ (**2a**)	117.04	2.613
$[(Br)(PhCH_2)As\{Cr(CO)_5\}_2]^-$ (**3**)	124.00	2.509
$[HSb\{Cr(CO)_5\}_3]^{2-}$ (**2b**)	116.88	2.735
$[Cl_2Sb\{Cr(CO)_5\}_2]^-$ (**7**)	129.01	2.585
$[BrISb\{Cr(CO)_5\}_2]^-$ (**8**)	132.96	2.624

distance in **2a** is the greatest because of the steric effect of the $Cr(CO)_5$ group. The average As−Cr bond length in **2a** is 2.613(1) Å, which is not only significantly longer than those of the As−Cr multiple bonds in $ClAs\{Cr(CO)_5\}_2$ (av 2.324(2) Å),[3] $PhAs\{Cr(CO)_5\}_2$ (av 2.385(3) Å),[3] $Mn(CO)_5As\{Cr(CO)_5\}_2$ (av 2.429(4) Å),[4] $Mn(CO)_5As(\mu\text{-}CO)\{Cr(CO)_4\}_2$ (av 2.349(5) Å),[4] and $(^tBu)As\{Cr(CO)_5\}_2$ (av 2.345(1) Å)[21] but also greater than those of the As−Cr single bonds in $[Et_4N]_2[$**1**$]$ (av 2.516(2) Å) and $As_2Cr_3Co_2(CO)_{20}$ (av 2.422(2) Å).[22] For **1** and **3**, the average As−Cr bond lengths are 2.516 and 2.509 Å, respectively, and are close to those of the reported As−Cr single bonds. The lengthening of the As−Cr bonds in **2a** is evident and caused by the steric crowding of the three chromium carbonyl fragments. On the other hand, the Cr−As−Cr bond angle increases as the number of the $Cr(CO)_5$ fragments decreases.

Similarly, of the Sb−Cr complexes **2b**, **7**, and **8**, the Sb−Cr distance is the greatest in **2b** and similar to those in **7** and **8**. The average Sb−Cr bond length in $[Et_4N]_2[$**2b**$]$ is 2.735(2) Å, which is larger than those of the Sb−Cr multiple bonds in $[Sb\{Cr(CO)_5\}_3]^-$ (av 2.630(3) Å)[4] and that in $[SbFe_3Cr(CO)_{17}]^-$ (2.6382(9) Å).[23] However, the Sb−Cr distances in **7** and **8** (2.585(2), 2.624(1) Å) are normal. The lengthening of these Sb−Cr bonds in **2b** is again influenced by the steric crowding of the three chromium carbonyl fragments. As shown, the steric effect of the substituents on the Sb atoms is also reflected in the trends of the Cr−Sb−Cr angles.

Conclusion

We have developed a facile route to a new series of group 15−chromium carbonyl hydrido complexes $[H_2As\{Cr(CO)_5\}_2]^-$ and $[HE\{Cr(CO)_5\}_3]^{2-}$ (E = As, Sb). The contrasting reactivity patterns of the dianionic hydrido complexes $[HE(Cr(CO)_5)_3]^{2-}$ (E = As, Sb) toward organic halogen derivatives are demonstrated. While the reaction of $[HAs\{Cr(CO)_5\}_3]^{2-}$ with RX yields the RX addition products $[(R)(X)As\{Cr(CO)_5\}_2]^-$, the treatment of $[HSb\{Cr(CO)_5\}_3]^{2-}$ with RX forms the halo-substituted complexes $[XSb\{Cr(CO)_5\}_3]^{2-}$ probably because of the greater ease of toleration of the higher negative charge of the resultant complexes by the larger Sb atom. The hydrogen-transferring efficiency of $[HE(Cr(CO)_5)_3]^{2-}$ (E = As, Sb) with RX to form R−H is comparable under our conditions. Additionally, the interesting dihaloantimony complexes $[XX'Sb\{Cr(CO)_5\}_2]^-$ can be obtained from the reaction of $[HSb(Cr(CO)_5)_3]^{2-}$ with the appropriate organic halides.

Acknowledgment. We thank the National Science Council of the Republic of China for financial support (Grant NSC 88-2113-M-003-013)

Supporting Information Available: X-ray crystallographic files in CIF format for complexes $[Et_4N][$**1**$]$, $[Et_4N]_2[$**2a**$]$, $[Et_4N]_2[$**2b**$]$, $[Et_4N][$**3**$]$, $[Et_4N][$**7**$]$, and $[Bu_4N][$**8**$]\cdot 0.5CH_2Cl_2$. This material is available free of charge via the Internet at http://pubs.acs.org.

IC0004277

---

(21) Jones, R. A.; Whittlesey, B. R. *Organometallics* **1984**, *3*, 469.

(22) Lang, H.; Huttner, G.; Sigwarth, B.; Jibril, I.; Zsolnai, L.; Orama, O. *J. Organomet. Chem.* **1986**, *304*, 137.

(23) Whitmire, K. H.; Shieh, M.; Cassidy, J. *Inorg. Chem.* **1989**, *28*, 3164.